Int J Clin Exp Med 2018;11(7):7004-7017
www.ijcem.com /ISSN:1940-5901/IJCEM0069480

Original Article

Identification of commonly regulated genes and biological pathways as potential targets in PC-3 and DU145 androgen-independent human prostate cancer cells treated with the curcumin analogue 1,5-bis(2-hydroxyphenyl)-1,4-pentadiene-3-one

Kamini Citalingam[1], Faridah Abas[2,3*], Nordin H Lajis[2*], Iekhsan Othman[1*], Rakesh Naidu[1*]

[1]Jeffery Cheah School of Medicine and Health Sciences, Monash University Malaysia, Jalan Lagoon Selatan, 47500 Bandar Sunway, Selangor, Malaysia; [2]Laboratory of Natural Products, Faculty of Science, [3]Department of Food Science, Universiti Putra Malaysia, 43400 UPM Serdang, Selangor, Malaysia. [*]Equal contributors.

Received November 20, 2017; Accepted May 3, 2018; Epub July 15, 2018; Published July 30, 2018

Abstract: Diarylpentanoid [1,5-bis(2-hydroxyphenyl)-1,4-pentadiene-3-one] (MS17) demonstrated enhanced anticancer activity compared to curcumin but its effect on androgen-independent prostate cancer has not been well-studied. The present study was aimed to perform gene expression profiling on MS17 treated PC-3 and DU145 cells using microarray technology to identify mutually regulated genes as common targets in both androgen-independent prostate cancer cell lines as well as molecular pathways that contributes to the anticancer activity of MS17. The profiling data revealed a dose-dependent gene regulation, evident by higher fold change expression values when the treatment dose was increased by 1.5-fold in both cell lines. Gene ontology classification was performed on highly regulated differentially expressed genes (DEGs). Among these genes, the mutually regulated DEGs were identified as common targets in both cell lines. The mutually up-regulated DEGs included, *CRYAB* and *DNAI2* associated with cytoskeletal organization, *HSPA6* and *HSPB8* with response to unfolded protein, *MMP3* and *MMP10* with proteolysis, *CACNA1G* with transporter activity, *NGFR* with apoptosis, *CCL26* with immune response, *DNAJA4* with protein folding and *TRIML2* with protein ubiquitination. However, the down-regulated genes such as *CTDSP1* were associated with phosphatase activity, *HIST1H2BF* and *HIST1H2AI* with chromosome organization, *MXD3* with regulation of transcription and *TNFRSF6B* with apoptosis. PC-3 and DU145 are androgen-independent prostate cancer cells with different biological properties, and identification of common targets in both cell lines could potentially be used as therapeutic targets. Pathway analysis of the DEGs in PC-3 cells demonstrated modulation of top pathways associated with cell cycle checkpoint, DNA damage, and inflammatory response while in DU145 cells the pathways were associated with immune response and metabolism. Thus, the findings of the present study provide insight into the antitumor activity of MS17 and as a potential chemotherapeutic agent for androgen independent prostate cancer cells.

Keywords: Androgen-independent prostate cancer, diarylpentanoid, microarray gene expression profiling, pathway analysis

Introduction

Prostate cancer is the leading cause of cancer among men. Although in the initial stage prostate cancer cells responds well to androgen deprivation therapy, it often progresses to an androgen-independent phenotype that is resistant to treatment [1]. Despite available therapeutic options, much effort has been directed towards developing novel treatment modalities to prevent the progression of hormone sensitive prostate cancer cells to hormone refractory stage. Curcumin, a polyphenol active compound extracted from the rhizome of the turmeric plant, *Curcuma longa* has known to demonstrate potential anticancer effect against a variety of carcinomas both *in vitro* and *in vivo* [2]. Despite the success of curcumin in treating cancer, its poor pharmacokinetic characteristics stimulated chemists to synthesize variety

of analogues with the hope to obtain compounds that are more effective and with a wider spectrum of anti-tumor activity while retaining its safety profile [3-5]. Diarylpentanoids (DAPs), a group of curcumin-like analogues with 5-carbon chain between its aryl rings was reported to display significant growth suppressive potential compared to curcumin [6]. Several studies have demonstrated anticancer activity of DAPs in a wide range of cancer cell lines [7-12]. EF-24 [3,5-bis(2-fluorobenzylidene)-4-piperidone] a curcumin DAP exhibited potent growth inhibitory effects in a variety of cancer cells including prostate cancer at doses significantly lower than curcumin [13]. Other investigators reported the anti-tumorigenic effects of the structurally identical DAP ca27 and Ca 37 in androgen-dependent and -independent prostate cancer cells respectively [7, 14]. While many of these DAPs demonstrated an improved anticancer effect compared to curcumin, the underlying mechanisms that contributed to its anticancer activity in prostate cancer cells remains to be explored.

In our recent study, curcumin diarylpentanoid 1,5-Bis(2-hydroxyphenyl)-1,4-pentadiene-3-one (MS17) demonstrated improved dose- and time-dependent growth inhibitory effects on androgen-independent prostate cancer cell lines, PC-3 and DU145 respectively at EC_{50} values of approximately 5.0 μM compared to curcumin. MS17 also demonstrated significant apoptotic effects at 24 hours of treatment with early apoptosis noted at 2 × EC_{50} (10 μM) and 3 × EC_{50} (15 μM) concentrations in the treated cells [15]. Hence, in the present study we performed gene expression profiling on MS17 treated PC-3 and DU145 cells using microarray technology to identify mutually regulated genes as common targets in both androgen-independent prostate cancer cell lines as well as molecular pathways that contributes to the anticancer activity of MS17.

Materials and methods

Cell culture and preparation of MS17 diarylpentanoid

Androgen-independent metastatic human prostate cancer cell line, PC-3 and DU145 cells were purchased from American Type Culture Collection (ATCC, Rockville, MD, USA) and cultured as previously described [15]. Separately, the chemically purified diarylpentanoid, MS17 [1,5-Bis(2-hydroxyphenyl)-1,4-pentadiene-3-one] was synthesized based on the method described previously [16], and was prepared by dissolving in 100% DMSO (Sigma-Aldrich, St. Louis, MO, USA) to a final concentration of 50 mM.

Treatment and total RNA isolation

Cells were seeded in triplicate wells containing 4 × 10^5 cells/mL in 6-well tissue culture plates and treated with 10 μM and 15 μM doses of MS17 for 24 hours. Control wells (untreated cells) containing media only with 0.5% DMSO was also included. Following overnight incubation, cells were harvested and RNA was isolated using RNeasy® Mini Kit (Qiagen, Valencia, CA, USA) and purified using RNase-free DNA set according to the manufacturer's protocol. Concentration and purity of the extracted RNA was measured spectrophotometrically using NanoDrop 1000 (Thermo Fisher Scientific, Waltham, MA, USA). RNA integrity was assessed using Agilent 2100 Bioanalyzer (Agilent Technologies, Santa Clara, CA, USA) and scored as RNA integrity number (RIN). Samples with RIN score exceeding 8 indicate high RNA quality and were selected for microarray analysis.

Microarray

Genome-wide expression profiles of the treated and untreated samples were analyzed using Agilent one-color microarray-based gene expression analysis protocols (Agilent Technologies). Briefly, 100 ng quality-checked total RNA was reverse transcribed using a Low Input Quick Amp labeling kit and then transcribed to Cy3-labeled cRNA according to the manufacturer's protocol. Cy3-labeled cRNA samples were hybridized onto whole human genome SurePrint G3 8X60K arrays (Agilent Technologies) using Agilent's Surehyb Chambers in an Agilent hybridization oven set at 65°C for 17 hours. Three independent replicates were performed for each treatment. The slides were washed and subsequently scanned by an Agilent G2600D SureScan Microarray Scanner (Agilent Technologies). Images from the scanned array were analyzed using Agilent's Feature Extraction software, version 11.5.1.1 and further analyzed for statistical evaluations using GeneSpring GX version-13.0 software (Agilent Technologies).

Data normalization and statistical analysis

Data normalization and transformation steps recommended by Agilent Technologies for one-color oligonucleotide microarrays were performed using GeneSpring GX software. The raw signals were log transformed and normalized using the Percentile shift normalization method. Quality control on the probe sets were filtered based on flag and expression values to remove probes with low signal intensities (< 20.0). Statistical comparisons were performed between the experimental groups by using Analysis of Variance (ANOVA) with Benjamini-Hochberg false discovery rate (FDR) set as a multiple test correction method, followed by a post hoc testing using Turkey's Honestly Significance Difference (HSD) to identify pair-wise significant genes. Genes that exhibited corrected *p*-value < 0.05 and a fold change (FC) in expression greater than 2.0 (FC > 2.0 denotes up-regulation; FC < -2.0 denotes down-regulation) compared to control cells were identified as being differentially expressed genes (DEGs).

Gene Ontology (GO) classification analysis

Specific FC cut-off values (PC-3; up-regulated DEGs = FC ≥ 18.0 while down-regulated DEGs = FC ≤ -3.7 and DU145; up-regulated DEGs = FC ≥ 15 while down-regulated DEGs = FC ≤ -2.5) were applied to the list of DEGs to obtain a list of top ranked DEGs that were under/over expressed by treatment. Hierarchical cluster analysis for the top ranked DEGs was performed to demonstrate the response to treatment by MS17. Gene Ontology (GO) analysis was also performed on the highly regulated genes using The Database for Annotation, Visualization and Integrated Discovery (DAVID) functional annotation tool (htpp://david.abcc.ncifcrf.gov) version 6.7. The selected genes were categorized based on GO functional category to provide a description of the biological process (BP)/ molecular function (MF) and their corresponding GO terms were identified.

Pathway analysis

The list of DEGs that were obtained from the microarray analysis which satisfied the *p*-value < 0.05 and FC cut-off criteria were selected for pathway analysis based on a database of curated pathways. Gene symbols were imported into Ingenuity® Pathway Analysis (IPA) software (IPA®; QIAGEN Redwood City, www.qiagen.com/ingenuity) and DEG's from the prostate cancer cells were mapped to canonical pathways using reference genes from the Ingenuity Knowledge Base. Using the Fishers Exact Test the *p*-value was set at $p < 0.05$, canonical pathways were considered as statistically significant when it passed through a threshold of 1.3 [calculated by -log (*p*-value)]. A ratio value calculating the number of genes from the dataset that matched components within the pathway was also calculated.

Real-time PCR (qRT-PCR) validation

Selected candidate genes which was previously identified by microarray analysis at 24 hours, were validated by qRT-PCR. The total RNA which was used for microarray analysis were reverse transcribed to cDNA using the High-Capacity cDNA Reverse Transcription kit according to the manufacturer's specifications (Applied Biosystems). The cDNA was then used as templates for PCR amplification of selected genes using the TaqMan probes. A set of 6 genes were used to validate gene expression in PC-3 and DU145 cells which includes *MMP3* (Hs00968308_m1), *MMP10* (Hs00233987_m1), *CCL26* (Hs00171146_m1), *CTDSP1* (Hs01105503_m1), *MXD3* (Hs00361007_m1) and *TNFRSF6B* (Hs00187070_m1). *GAPDH* (Hs99999905_m1) was used as the internal control. Each sample was run in duplicates in a final volume of 20 µL. The reactions were carried out using a StepOnePlus™ Real-time PCR system (Applied Biosystems) and the cycling program was set as follows: an initial PCR activation step at 48°C for 30 min followed by 95°C for 10 min. 40 cycles of melting at 95°C for 15 s and annealing/extension at 60°C for 1 min. Relative gene expression was calculated using the comparative C_T method ($\Delta\Delta C_T$). Expression was reported as fold change in the level of mRNA of treated cells relative to untreated cells, normalized to *GAPDH* expression value. Histograms and statistical analysis were performed using Graphpad Prism version 5.04 for Windows (Graphpad Software, La Jolla, CA, USA).

Results

Gene expression profiling and Gene Ontology (GO) classification analysis

The gene expression data identified a total of 7429 and 4252 significant ($p < 0.05$) entities in

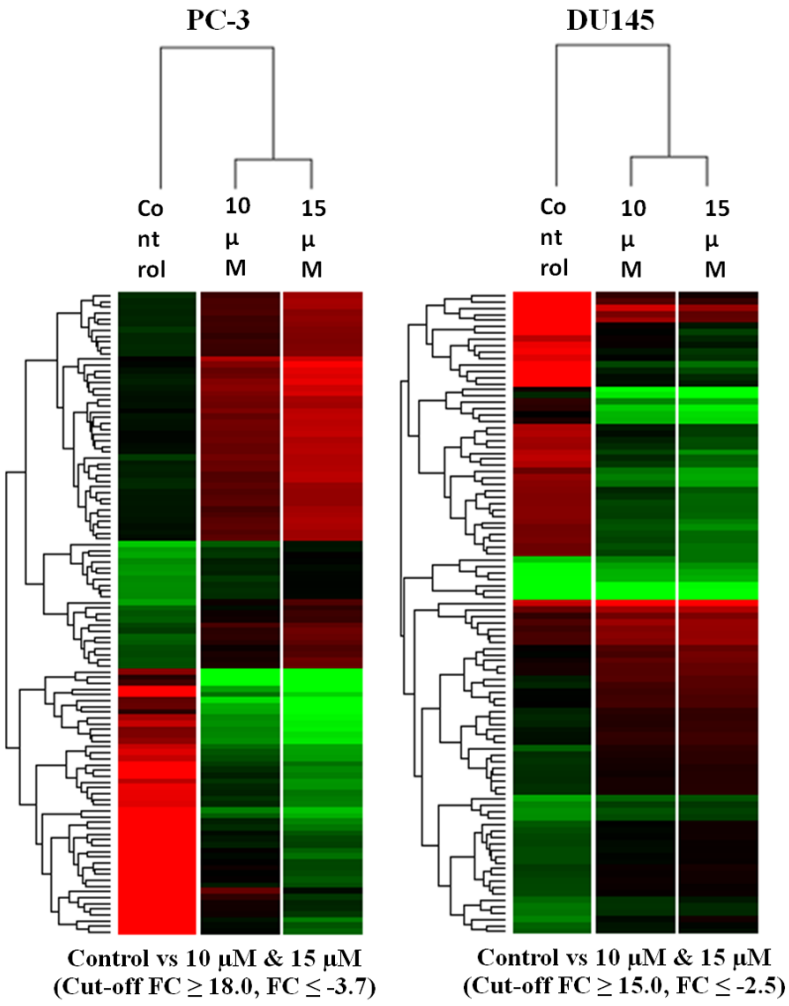

Figure 1. Hierarchical cluster analysis of top deregulated DEGs in MS17-treated PC-3 and DU145 cells as compared to control cells. Specific cut-off values were applied to each group of genes and the hierarchical clustering was generated based on the cut-off criteria. Overall, the hierarchical cluster analysis revealed significant differences between the MS17-treated and control groups in both cell lines. The regulation pattern was differentiated with 2 distinct colors; green indicates up-regulation while red represents down-regulation and black corresponds to intermediate regulation relative to control cells.

PC-3 and DU145 cells respectively. Of these, 1386 genes in PC-3 and 987 genes in DU145 cells were differentially expressed in response to 10 μM and 15 μM treatment of MS17. Among these genes, a total of 33 up- and 56 down-regulated genes were obtained in PC-3 cells (Supplementary Table 1) while 32 up- and 49 down-regulated genes were identified as the top ranked DEGs in MS17-treated DU145 cells (Supplementary Table 2). The top deregulated genes were graphically represented by hierarchical clustering to view the changes in the gene expression patterns (**Figure 1**).

Overall, it was noted that an increase in treatment dosage by 1.5-fold from 10 μM to 15 μM resulted in significant increase in expression levels by several fold, proposing a dose-dependent pattern of gene regulation by MS17 in the prostate cancer cells. Based on Gene Ontology (GO) classification analysis, a total of 19 and 22 functional categories were identified in PC-3 and DU145 cells, respectively. Among the total of 19 functional categories in PC-3 cells, cytoskeletal organization constituted the major proportion (16%) followed by cell cycle (15%), chromosome organization (12%), regulation of transcription (10%) and binding activity (6%). However, the rest of the functional categories represented approximately 1-4% of the DEGs (**Figure 2A**). Amongst the 22 functional categories associated with DU145 cells, the largest functional category was regulation of transcription (11%) followed by oxidoreductase activity, binding activity, and transporter activity each comprised of 10%, while metabolic process accounts for 9%, signal transduction activity for 7% and apoptosis for 5% of the DEGs. However, the other functional categories constitues between 1-4% of the DEGs (**Figure 2B**).

Among the total DEGs, 11 up- and 5 down-regulated genes in PC-3 and DU145 cells were identified as mutually regulated genes in both dosages as well as common gene targets of MS17 in both the cell lines. The selected genes from both cell lines along with their corresponding functional categories are highlighted in **Table 1**. Among these 3 up- and 3 down-regu-

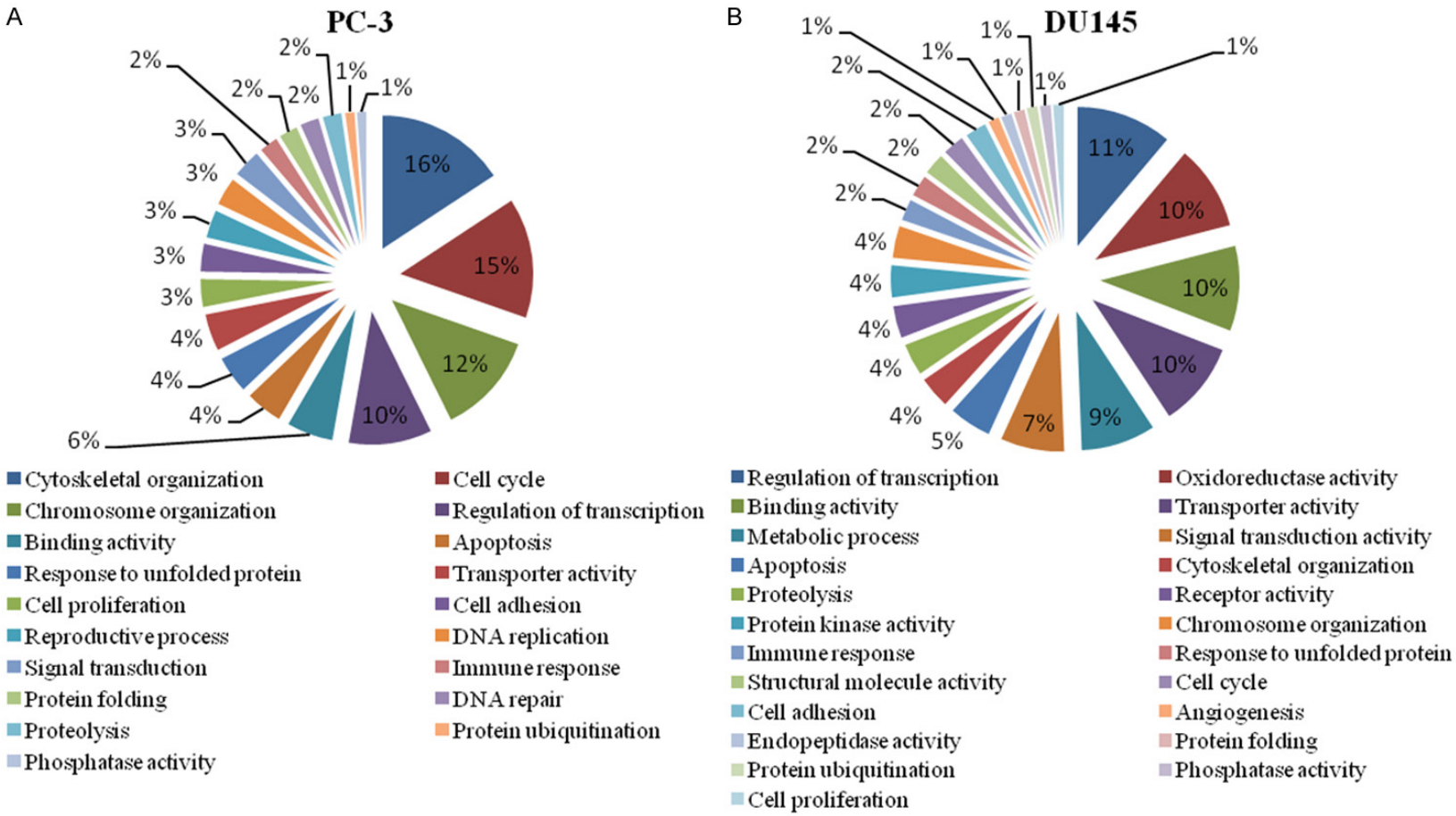

Figure 2. Gene Ontology (GO) classification of the top deregulated DEGs in (A) PC-3 and (B) DU145 cells.

Table 1. Selected differentially expressed genes (DEGs) mutually regulated following 10 μM and 15 μM treatment of MS17 in PC-3 and DU145 cells at 24 hrs

GO Term/ Gene Symbol	Genbank accession	Gene description	PC-3			DU145		
			FC (10 μM)	FC (15 μM)	*p*-Value	FC (10 μM)	FC (15 μM)	*p*-Value
Up-regulated								
Cytoskeletal organization								
*CRYAB**	NM_001885	Crystallin, alpha B	277.6	537.6	5.42E-04	334.9	493.9	5.46E-04
*DNAI2**	NM_023036	Dynein, axonemal, intermediate chain 2	24	51.9	7.84E-03	17.6	32.1	3.77E-02
Response to unfolded protein								
*HSPA6**	NM_002155	Heat shock 70 kDa protein 6 (HSP70B')	145.2	336.7	1.09E-03	373.4	814.4	4.96E-04
*HSPB8**	NM_014365	Heat shock 22 kDa protein 8	41.3	88.4	1.67E-03	12	18	2.89E-02
Protein ubiquitination								
*TRIML2**	NM_173553	Tripartite motif family-like 2	30.2	88.1	6.54E-03	11.6	24.7	3.61E-02
Transporter activity								
*CACNA1G**	NM_018896	Calcium channel, voltage-dependent, T type, alpha 1G subunit	17	48.3	2.51E-03	23	60.2	3.60E-02
Proteolysis								
*MMP3**	NM_002422	Matrix metallopeptidase 3 (stromelysin 1, progelatinase)	15.6	33.9	2.92E-03	71.6	122.8	5.83E-03
*MMP10**	NM_002425	Matrix metallopeptidase 10 (stromelysin 2)	9.2	20.9	6.03E-03	96.7	165.2	5.11E-03
Protein folding								
*DNAJA4**	NM_018602	DnaJ (Hsp40) homolog, subfamily A, member 4	16.3	31.7	1.55E-03	11.5	19.1	3.87E-03
Apoptosis								
*NGFR**	NM_002507	Nerve growth factor receptor	14.2	23.8	6.34E-03	31.5	53.6	1.15E-02
Immune response								
*CCL26**	NM_006072	Chemokine (C-C motif) ligand 26	13	23.1	1.51E-03	56	81.4	1.70E-03
Down-regulated								
Phosphatase activity								
*CTDSP1**	NM_021198	CTD (carboxy-terminal domain, RNA polymerase II, polypeptide A) small phosphatase 1	-5.8	-9.3	6.59E-04	-4.7	-5.8	6.10E-03
Chromosome organization								
*HIST1H2AI**	NM_003509	Histone cluster 1, H2ai	-3.7	-5.7	1.66E-03	-2.6	-2.8	3.15E-03
*HIST1H2BF**	NM_003522	Histone cluster 1, H2bf	-3.5	-4.6	1.88E-03	-2.7	-3.3	2.38E-02
Apoptosis								
*TNFRSF6B**	NM_003823	Tumor necrosis factor receptor superfamily, member 6b, decoy	-3.4	-4	2.10E-02	-4.5	-6.5	3.66E-03
Regulation of transcription								
*MXD3**	NM_031300	MAX dimerization protein 3	-2.6	-3.7	4.18E-03	-2	-2.7	1.02E-02

*Green represents mutually up-regulated genes while red indicates mutually down-regulated genes.

Table 2. Top 5 Canonical pathways significantly modulated by mutually deregulated DEGs in 10 μM- and 15 μM-treated prostate cancer cells

Canonical pathways	Nominal *p*-value	*Genes
PC-3		
Mitotic Roles of Polo-Like Kinase	1.58E-05	*CCNB2*, *FBXO5*, *PLK1*, *CDK1*, *KIF11**
Cell Cycle: G2/M DNA Damage Checkpoint Regulation	9.55E-05	*TOP2A*, *CCNB2*, *PLK1*, *CDK1**
Granulocyte Adhesion and Diapedesis	2.29E-04	*CLDN11*, *MMP3*, *MMP10*, *CCL26**
Agranulocyte Adhesion and Diapedesis	2.88E-04	*CLDN11*, *MMP3*, *MMP10*, *CCL26**
ATM Signaling	2.40E-03	*CCNB2*, *BLM*, *CDK1**
DU145		
Airway Pathology in Chronic Obstructive Pulmonary Disease	7.94E-03	*MMP1**
Zymosterol Biosynthesis	2.00E-02	*TM7SF2**
Guanosine Nucleotides Degradation III	2.40E-02	*NT5E**
Urate Biosynthesis/Inosine 5'-phosphate Degradation	3.16E-02	*NT5E**
Dermatan Sulfate Biosynthesis (Late Stages)	3.16E-02	*CHST1**

Note: Green represents mutually up-regulated genes while red indicates mutually down-regulated genes.

lated genes were seletced for validation using qRT-PCR. The mutually up-regulated genes included, *CRYAB* and *DNAI2* were associated with cytoskeletal organization, *HSPA6* and *HSPB8* with response to unfolded protein, *MMP3* and *MMP10* with proteolysis, *CACNA1G* with transporter activity, *NGFR* with apoptosis, *CCL26* with immune response, *DNAJA4* with protein folding and *TRIML2* with protein ubiquitination. Analysis of the mutually repressed DEGs demonstrated down-regulation of *CTDSP1* associated with phosphatase activity, *HIST1H2BF* and *HIST1H2AI* with chromosome organization, *MXD3* with regulation of transcription and *TNFRSF6B* with apoptosis.

Pathway analysis of the MS17 treated prostate cancer cells

The top deregulated DEGs were mapped to biological canonical pathways to identify and understand the cellular pathways that significantly modulated by MS17 treated prostate cancer cells. The top 5 canonical pathways of PC-3 and DU145 cells that were significantly induced/activated by treatment were selected for further analysis. For each pathway, the respective nominal *p*-value along with all the input genes are presented in **Table 2**.

In PC-3 cells, the most significantly activated pathway, Mitotic Roles of Polo-Like Kinase was associated with the down-regulation of *CCNB2, FBXO5, PLK1, CDK1,* and *KIF11* while the second most significantly activated pathway, Cell Cycle: G2/M DNA Damage Checkpoint Regulation was modulated by down-regulation of *TOP2A, CCNB2, PLK1,* and *CDK1* expression. In addition, Granulocyte Adhesion and Diapedesis, and Agranulocyte Adhesion and Diapedesis pathways were modulated by induced expression of *MMP3, MMP10,* and *CCL26* and down-regulation of *CLDN11* respectively. Conversely, the fifth ranking pathway, ATM signaling was modulated by the suppressed expression of *CCNB2, BLM,* and *CDK1*.

On the other hand, the two most significantly activated pathways in DU145 cells; Airway Pathology in Chronic Obstructive Pulmonary Disease and Zymosterol Biosynthesis were associated with the induction of *MMP1* and repression of *TM7SF2* respectively. The pathways, Guanosine Nucleotides Degradation III and Urate Biosynthesis/Inosine 5'-phosphate Degradation was modulated by the down-regulation of *NT5E* respectively. In addition, Dermatan Sulfate Biosynthesis (Late Stages) was associated with the up-regulation of *CHST1* expression.

Validation of selected MS17-regulated genes using qRT-PCR

To substantiate the results from the microarray analysis, quantitative real-time PCR (qRT-PCR) was performed to validate the expression of six selected MS17 mutually expressed genes in the prostate cancer cells. The expression data from real-time PCR was normalized against the housekeeping gene, *GAPDH* and both results

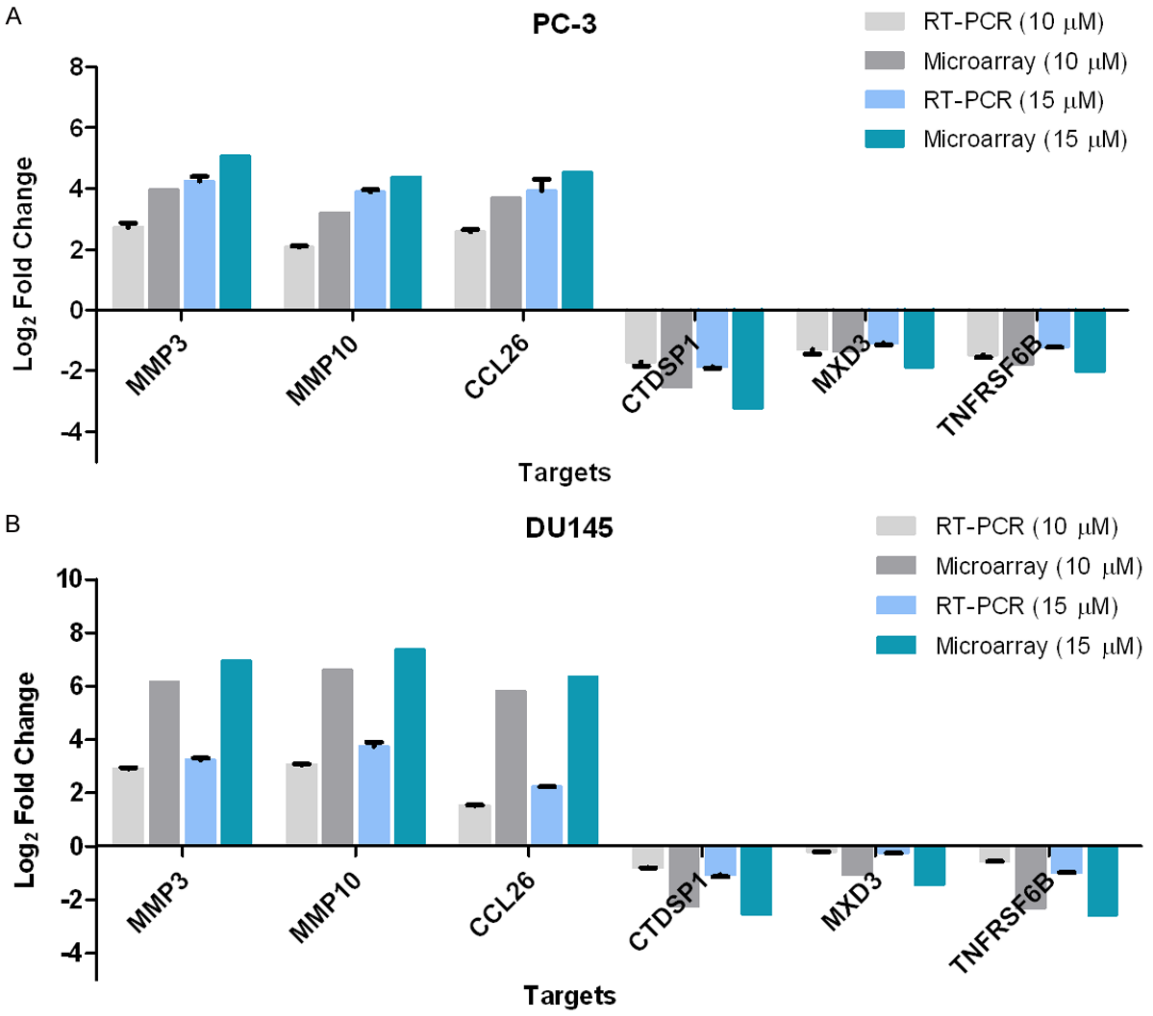

Figure 3. mRNA expression of selected genes from microarray analysis was confirmed using qRT-PCR. cDNA from MS17-treated (A) PC-3 and (B) DU145 cells from 3 independent experiments were used for validation of the gene expression obtained from microarray analysis. The selected up-regulated genes were *MMP3, MMP10,* and *CCL26* while the down-regulated genes were *CTSPD1, MXD3,* and *TNFRSF6B.* Data was presented as $\log_2$ fold change in MS17-treated cells as compared to untreated cells. All data were normalized to the housekeeping gene, *GAPDH*. Results show that the expression patterns obtained through real-time PCR were consistent with the microarray results.

were expressed as $\log_2$ fold change in MS17-treated cells compared to untreated cells. Validation confirmed up-regulation of *MMP3, MMP10,* and *CCL26* and down-regulation of *CTSPD1, MXD3,* and *TNFRSF6B* gene expressions in both MS17-treated PC-3 and DU145 cells, which were consistent with the microarray data (**Figure 3**).

Discussion

In the present study, PC-3 and DU145 cells were used as a model of androgen-independent human prostate cancer cells. PC-3 cells were derived from bone metastasis with high metastatic potential harbours wild-type p53 while DU145 cells were derived from brain metastasis and moderately metastatic with mutant p53. Despite the biological differences, we identifed mutually regulated DEGs as common targets in both cell lines and DEGs mapped to relevant cellular pathways, and their role in anticancer activity were discussed.

CRYAB and *HSPA6* associated with cytoskeletal organization and response to unfolded protein respectively were the topmost over-expressed transcripts and particularly relevant due to their mutual up-regulation in both MS17-treated prostate cancer cells. *CRYAB* encodes alpha-B crystalline protein which is a heat-shock protein and molecular chaperone that

participates in intracellular architecture of the cytoskeleton. *CRYAB* is a potential tumor-suppressor gene and over-expression of *CRYAB* suppressed nasopharyngeal carcinoma tumorigenicity *in vivo* by affecting cell adhesion, migration, and interaction with tumor microenvironment while its decreased expression correlated with cancer progression [17]. Heat shock proteins (HSPs) are powerful molecular chaperones that play central role in the correct folding of misfolded protein and drive damaged proteins to endoplasmic reticulum for proteasome degradation in conditions of cellular oxidative stress [18]. *HSPA6* codifies for the stress inducible Hsp70B' protein that plays a key role in mediating cell survival during endoplasmic reticulum stress condition. Induced *HSPA6* expression by curcumin analogue D6 in melanoma cells caused cellular toxicity and endoplasmic reticulum stress that resulted in apoptotic cell death [19]. In addition, induction of apoptosis in human schwannoma cell line exposed to curcumin treatment was associated with up-regulation of Hsp70 [20]. Apart from *HSPA6*, *HSPB8* was also mutually up-regulated by 2.3- and 2.1-fold respectively when treatment dose was increased by 1.5-fold in PC-3 and DU145 cells. *HSPB8* is silenced by aberrant DNA methylation in a high proportion of melanoma prostate cancer, Ewing's sarcoma and hematologic malignancies. However, its expression induces cell death and inhibits tumor growth in xenograft models suggesting *HSPB8* could be a tumor suppressor [21]. Curcumin was shown to induce heat shock response in human cervical cancer and colorectal carcinoma cells [22-24]. Therefore, induction of these transcripts during endoplasmic stress may contribute to apoptosis and suppress tumor formation. *DNAJA4* associated with protein folding encodes for heat shock protein family Hsp40 which is a metastatic suppressor gene. *DNAJA4* promotes Apolipoprotein E (ApoE) expression, an anti-angiogenic and metastasis-suppressive factor in melanoma cells resulting in suppression of melanoma metastasis [25]. Endogenous ApoE and *DNAJA4* were found to suppress metastatic endothelial recruitment *in vivo* [25]. The increase expression of this transcript by MS17 may induce apoptosis and mediate anti-metastatic activity in the treated cells.

In addition to *CRYAB*, *DNAI2* was also associated with cytoskeletal organization. *DNAI2* is a part of the large minus end-directed microtubule motor complex and associated with the dynein complex. It is involved in ciliogenesis and associated with cell motility [26, 27]. In mitosis, dynein participates in chromosome movements, spindle organization, spindle positioning, and checkpoint silencing [26, 27]. Up-regulation of *DNAI2* and the cytoskeletal-related genes by MS17 suggests a potential role in maintaining the cytoskeletal architecture of the prostate cancer cells and inhibition may reduce the cytoskeletal organization and increase tumor cell motility.

Transcripts associated with proteolysis such as *MMP10* and *MMP3* were significantly induced in response to treatment. Metallopeptidases (MMPs) are known as the collagenase-related connective tissue degrading MMPs that are associated with proteolytic degradation of the ECM during inflammation and immune response [28]. MMPs were shown to play dual roles in oncogenesis, either as oncogenes or as tumor-suppressors. *MMP10* is associated with proteolytic degradation of the ECM during inflammation and immune response [29]. In contrast, depletion in *MMP3* expression in squamous cell carcinoma tumors *in vivo* stimulated tumorigenesis and was associated with leukocyte infiltration [30]. Induction of specific MMPs by MS17 proposes that it may participate in the proteolytic ECM degradation and host defence mechanism of the treated prostate cancer cells to exert its anti-cancer effect.

CACNA1G and *NGFR* associated with transporter activity and apoptosis respectively, were mutually up-regulated in both prostate cancer cells. *CACNA1G* codifies a T-type calcium channel protein which regulates cytosolic calcium during cell proliferation and cell death. It has been reported that intracellular calcium signalling plays an important role in apoptosis [31]. Up-regulation of *CACNA1G* expression in cancer cells induces apoptosis and anti-proliferative activity [32]. *NGFR*, a transmembrane glycoprotein from the neurotrophin family was reported to act as a tumour suppressor. Up-regulation of *NGFR* expression in breast cancer cells facilitates anti-tumorigenesis, by negatively regulating cell proliferation and cancer cell growth [33]. Up-regulation of *CACNAIG* and *NGFR* by MS17 may suppress tumorigenesis by inducing anti-proliferative activity and apoptosis in prostate cancer cells, thus inhibiting cancer progression.

TRIML2 associated with protein ubiquitination is a member of a large tri-partite motif (TRIM) protein family that are implicated in transcriptional regulation, DNA damage, apoptosis, and cancer [34]. Increased expression of *TRIML2* in colorectal cancer cells enhanced the activation of pro-apoptotic target genes while its down-regulation impaired apoptotic induction [35]. Increased expression of *TRIML2* by MS17 may potentially suppress tumorigenesis and contribute toward pro-apoptotic activity in prostate cancer cells. The immune response-related gene, *CCL26* was also mutually up-regulated by treatment. *CCL26* is a member of the CC Chemokine family that encodes for dendritic-cell specific chemokines that are implicated in innate and acquired immune responses [36]. However its role in anti-tumorigenesis is yet to be known and requires further investigation.

In contrast to the up-regulated genes, several mutually repressed DEGs were also identified in both MS17 treated prostate cancer cells. *TNFRSF6B* associated with apoptosis is a soluble decoy receptor from the TNFR super-family which plays a regulatory role in suppressing FasL- and LIGHT-mediated cell death. *TNFRSF6B* induction in liver carcinoma cells correlated with metastasis while its down-regulation resulted in decreased cancer cell proliferation, activation of cell cycle arrest at G1/S phase, inhibition of cell migration and induction of apoptosis [37]. Over-expression of *TNFRSF6B* in colorectal cancer cells correlated with tumor differentiation, lymph node metastasis and overall poor patients survival [38]. In addition, down-regulation of *TNFRSF6B* expression in breast cancer cells inhibited cellular migration and invasion [39]. The down-regulation of *TNFRSF6B* expression by MS17 may inhibit cell proliferation and migration, activate cell cycle arrest and induce apoptosis in prostate cancer cells. The nuclear phosphatase expressed by *CTDSP1* belongs to the protein of small C-terminal domain phosphatases that acts as a transcriptional regulator of neuronal gene where it is commonly associated with the silencing of neuronal gene expression [40]. This suggests a possible transcriptional regulatory role of *CTDSP1* in the inhibition of prostate cancer cell survival demonstrating the anti-tumorigenic activity of MS17.

HIST1H2BF and *HIST1H2AI* associated with chromosome organization encode for histone cluster proteins that are involved in chromosome segregation and alignment [41]. Over-expression of these transcripts in cancer tissues has been associated with oncogenesis [41]. While information on the anti-tumorigenic role of *HIST1H2AI* is not well described, increased *HIST1H2BF* expression in non-lung cancer cells significantly correlated with gemcitabine drug resistance [42]. The down-regulation of these genes by MS17 may enhance sensitivity towards treatment and modulate chromosome organization that impairs prostate cancer cell survival which requires further investigation. Conversely, repression of *MXD3* is associated with regulation of transcription and encodes a MAD family transcription factor whose expression was up-regulated in mouse and human medulloblastomas while demonstrating anti-proliferative activity and increased apoptosis [43], suggesting its possible role as pro-apoptotic factor and negative regulator of cell proliferation in the cancer cells.

In the present study we have identified several DEGs modulated by MS17 treated PC-3 and DU145 prostate cancer cells that were mapped to relevant biological canonical pathways. In addition to the common genes discussed, DEGs associated with pathways were exclusively noted in either PC-3 or DU145 cells. The top 5 canonical pathways that significantly activated in PC-3 cells were associated with cell cycle checkpoint, DNA damage response and inflammatory response. The pathways “Mitotic Roles of Polo-Like Kinase”, “Cell Cycle: G2/M DNA Damage Checkpoint Regulation” and “ATM Signaling” were modulated by the down-regulation of *CCNB2* and *CDK1.* In addition, *PLK1* was also mapped to “Mitotic Roles of Polo-Like Kinase” and “Cell Cycle: G2/M DNA Damage Checkpoint Regulation” pathways. All three transcripts are critical regulators of cell cycle progression. Down-regulation of *CCNB2* and *CDK1* demonstrated increased apoptosis and induction of anti-proliferative activity in cancer cells [44, 45] while decreased *PLK1* expression leads to cell cycle arrest, induction of apoptosis and tumor suppression in cancer cells [46]. Conversely, “Mitotic Roles of Polo-Like Kinase” pathway was also associated with the modulation of *FBXO5* and *KIF11* which plays a key role in mitosis. Over-expression of *FBXO5* promotes chromosome instability and the formation of solid cancers *in vivo* [47] while its down-regulation inhibited cell proliferation [48]. Down-

regulation of *KIF11,* a kinesin protein, in cancer cells promotes apoptosis [49]. In addition to these genes, Cell Cycle: G2/M DNA Damage Checkpoint Regulation" and "ATM Signaling" pathways were also modulated by the down-regulation of *TOP2A* and *BLM* respectively. *TOP2A* and *BLM* were associated with DNA replication, and down-regulation in cancer cells inhibits cell growth [50, 51]. In addition, "Granulocyte Adhesion and Diapedesis" and "Agranulocyte Adhesion and Diapedesis" pathways were associated with inflammatory response and modulated by up-regulation of *MMP3, MMP10*, *CCL26,* and down-regulation of *CLDN11* expression. The roles of *MMP3, MMP10,* and *CCL26* have been described previously. Meanwhile, *CLDN11* which belongs to the tetraspanin family of proteins are integral to the structure and function of tight junctions. Up-regulation of *CLDN11* expression promoted gastric cancer tumorigenesis but down-regulation inhibits cell growth [52]. Notably, the modulation of the abovementioned pathways by the target genes demonstrated anti-cancer role of MS17 in contributing to anti-proliferative, tumor suppressive and apoptotic properties in treated PC-3 cells.

Likewise, the modulation of the top five canonical pathways in DU145 cells demonstrated the activation of pathways associated with immune response and metabolism. The pathways, "Airway Pathology in Chronic Obstructive Pulmonary Disease" and "Dermatan Sulfate Biosynthesis (Late Stages)" were modulated by the induced expression of *MMP1* and *CHST1* respectively. The exact function of individual MMPs may vary from tissue remodelling, angiogenesis, wound healing to inflammation, but *MMP1* expression was shown to promote tissue remodeling-associated activity in cancer cells [28]. However, *CHST1* expression was induced in cancer patients undergoing chemotherapy treatment and demonstrated protective effect on cells from skin toxicity [53, 54]. In addition, "Zymosterol Biosynthesis" was modulated by down-regulation of *TM7SF2. NT5E* was down-regulated in both "Guanosine Nucleotides Degradation III" and "Urate Biosynthesis/Inosine 5'-phosphate Degradation" pathways. *TM7SF2* is an enzyme that participates in the regulation of cholesterol homeostasis and inflammatory responses [55]. Inhibition of *TM7SF2* expression in skin papilloma mouse showed reduced expression of genes associated with resistance to neoplastic transformation and alteration in the expression of proteins involved in epidermal differentiation [56]. Inhibition of *NT5E* expression in human breast cancer cells activated cell cycle arrest, induced apoptosis, and suppressed tumor growth [57]. Due to its anti-tumorigenic effects, the association of these transcripts in relation to "Airway Pathology in Chronic Obstructive Pulmonary Disease", "Zymosterol Biosynthesis", "Dermatan Sulfate Biosynthesis (Late Stages)", "Guanosine Nucleotides Degradation III" and "Urate Biosynthesis/Inosine 5'-phosphate Degradation" pathways suggest the potential role of MS17 to repress tumor growth and modulate cell cycle arrest as well as induction of apoptosis in treated DU145 cells.

Although PC-3 and DU145 are androgen-independent prostate cancer cells with differenet biological properties, we identified several genes mutually regulated by MS17 which could potentially be used as therapeutic targets for androgen-independent prostate cancer cells. These commonly regulated genes may inhibit cell proliferation, migration, metastases, and induce apoptosis in prostate cancer cells. The pathway analysis revealed genes mapped to the relevant biological pathways were mainly associated with cell cycle arrest, anti-proliferative activity, metabolism, or apoptotic cell death when treated with MS17. Thus the findings of the present study provides an insight into the antitumor activity of MS17 and as a potential chemotherapeutic agent for androgen independent prostate cancer.

Acknowledgements

This study was financially supported by the Fundamental Research Grant Scheme, (FRGS/1/2013/SKK01/MUSM/02/1) under the Ministry of Higher Education (MOHE), Malaysia.

The first author would like to acknowledge the support from the Ministry of Higher Education Malaysia for providing scholarship under the MyBrain (MyPhD) scheme.

Disclosure of conflict of interest

None.

Address correspondence to: Rakesh Naidu, Jeffery Cheah School of Medicine and Health Sciences, Monash University Malaysia, Jalan Lagoon Selatan, 47500 Bandar Sunway, Selangor, Malaysia. E-mail: kdrakeshna@hotmail.com

References

[1] Navarro D, Luzardo OP, Fernandez L, Chesa N and Diaz-Chico BN. Transition to androgen-independence in prostate cancer. J Steroid Biochem Mol Biol 2002; 81: 191-201.

[2] Aggarwal BB, Sundaram C, Malani N and Ichikawa H. Curcumin: the Indian solid gold. Adv Exp Med Biol 2007; 595: 1-75.

[3] Anand P, Kunnumakkara AB, Newman RA and Aggarwal BB. Bioavailability of curcumin: problems and promises. Mol Pharm 2007; 4: 807-818.

[4] Garcea G, Jones DJ, Singh R, Dennison AR, Farmer PB, Sharma RA, Steward WP, Gescher AJ and Berry DP. Detection of curcumin and its metabolites in hepatic tissue and portal blood of patients following oral administration. Br J Cancer 2004; 90: 1011-1015.

[5] Perkins S, Verschoyle RD, Hill K, Parveen I, Threadgill MD, Sharma RA, Williams ML, Steward WP and Gescher AJ. Chemopreventive efficacy and pharmacokinetics of curcumin in the min/+ mouse, a model of familial adenomatous polyposis. Cancer Epidemiol Biomarkers Prev 2002; 11: 535-540.

[6] Ohori H, Yamakoshi H, Tomizawa M, Shibuya M, Kakudo Y, Takahashi A, Takahashi S, Kato S, Suzuki T, Ishioka C, Iwabuchi Y and Shibata H. Synthesis and biological analysis of new curcumin analogues bearing an enhanced potential for the medicinal treatment of cancer. Mol Cancer Ther 2006; 5: 2563-2571.

[7] Fajardo AM, MacKenzie DA, Ji M, Deck LM, Vander Jagt DL, Thompson TA and Bisoffi M. The curcumin analog ca27 down-regulates androgen receptor through an oxidative stress mediated mechanism in human prostate cancer cells. Prostate 2012; 72: 612-625.

[8] Nagaraju GP, Zhu S, Wen J, Farris AB, Adsay VN, Diaz R, Snyder JP, Mamoru S and El-Rayes BF. Novel synthetic curcumin analogues EF31 and UBS109 are potent DNA hypomethylating agents in pancreatic cancer. Cancer Lett 2013; 341: 195-203.

[9] Cen L, Hutzen B, Ball S, DeAngelis S, Chen CL, Fuchs JR, Li C, Li PK and Lin J. New structural analogues of curcumin exhibit potent growth suppressive activity in human colorectal carcinoma cells. BMC Cancer 2009; 9: 99.

[10] Selvendiran K, Tong L, Bratasz A, Kuppusamy ML, Ahmed S, Ravi Y, Trigg NJ, Rivera BK, Kalai T, Hideg K and Kuppusamy P. Anticancer efficacy of a difluorodiarylidenyl piperidone (HO-3867) in human ovarian cancer cells and tumor xenografts. Mol Cancer Ther 2010; 9: 1169-1179.

[11] Zhu S, Moore TW, Lin X, Morii N, Mancini A, Howard RB, Culver D, Arrendale RF, Reddy P, Evers TJ, Zhang H, Sica G, Chen ZG, Sun A, Fu H, Khuri FR, Shin DM, Snyder JP and Shoji M. Synthetic curcumin analog EF31 inhibits the growth of head and neck squamous cell carcinoma xenografts. Integr Biol (Camb) 2012; 4: 633-640.

[12] Paulraj F, Abas F, Lajis NH, Othman I, Hassan SS and Naidu R. The curcumin analogue 1,5-Bis(2-hydroxyphenyl)-1,4-pentadiene-3-one induces apoptosis and downregulates E6 and E7 oncogene expression in HPV16 and HPV18-infected cervical cancer cells. Molecules 2015; 20: 11830-11860.

[13] Adams BK, Cai J, Armstrong J, Herold M, Lu YJ, Sun A, Snyder JP, Liotta DC, Jones DP and Shoji M. EF24, a novel synthetic curcumin analog, induces apoptosis in cancer cells via a redox-dependent mechanism. Anticancer Drugs 2005; 16: 263-275.

[14] Luo C, Li Y, Zhou B, Yang L, Li H, Feng Z, Li Y, Long J and Liu J. A monocarbonyl analogue of curcumin, 1,5-bis(3-hydroxyphenyl)-1,4-pentadiene-3-one (Ca 37), exhibits potent growth suppressive activity and enhances the inhibitory effect of curcumin on human prostate cancer cells. Apoptosis 2014; 19: 542-553.

[15] Citalingam K, Abas F, Lajis NH, Othman I and Naidu R. Anti-proliferative effect and induction of apoptosis in androgen-independent human prostate cancer cells by 1,5-bis(2-hydroxyphenyl)-1,4-pentadiene-3-one. Molecules 2015; 20: 3406-3430.

[16] Lee KH, Ab Aziz FH, Syahida A, Abas F, Shaari K, Israf DA and Lajis NH. Synthesis and biological evaluation of curcumin-like diarylpentanoid analogues for anti-inflammatory, antioxidant and anti-tyrosinase activities. Eur J Med Chem 2009; 44: 3195-3200.

[17] Huang Z, Cheng Y, Chiu PM, Cheung FM, Nicholls JM, Kwong DL, Lee AW, Zabarovsky ER, Stanbridge EJ, Lung HL and Lung ML. Tumor suppressor Alpha B-crystallin (CRYAB) associates with the cadherin/catenin adherens junction and impairs NPC progression-associated properties. Oncogene 2012; 31: 3709-3720.

[18] Oyadomari S, Araki E and Mori M. Endoplasmic reticulum stress-mediated apoptosis in pancreatic beta-cells. Apoptosis 2002; 7: 335-345.

[19] Rozzo C, Fanciulli M, Fraumene C, Corrias A, Cubeddu T, Sassu I, Cossu S, Nieddu V, Galleri G, Azara E, Dettori MA, Fabbri D, Palmieri G and Pisano M. Molecular changes induced by the curcumin analogue D6 in human melanoma cells. Molecular Cancer 2013; 12: 37-37.

[20] Angelo LS, Wu JY, Meng F, Sun M, Kopetz S, McCutcheon IE, Slopis JM and Kurzrock R. Combining curcumin (diferuloylmethane) and heat shock protein inhibition for neurofibroma-

tosis 2 treatment: analysis of response and resistance pathways. Mol Cancer Ther 2011; 10: 2094-2103.
[21] Aurelian L, Laing JM and Lee KS. H11/HspB8 and its herpes simplex virus type 2 homologue ICP10PK share functions that regulate cell life/death decisions and human disease. Autoimmune Dis 2012; 2012: 395329.
[22] Chen YC, Tsai SH, Shen SC, Lin JK and Lee WR. Alternative activation of extracellular signal-regulated protein kinases in curcumin and arsenite-induced HSP70 gene expression in human colorectal carcinoma cells. Eur J Cell Biol 2001; 80: 213-221.
[23] Dunsmore KE, Chen PG and Wong HR. Curcumin, a medicinal herbal compound capable of inducing the heat shock response. Crit Care Med 2001; 29: 2199-2204.
[24] Dikshit P, Goswami A, Mishra A, Chatterjee M and Jana NR. Curcumin induces stress response, neurite outgrowth and prevent NF-kappaB activation by inhibiting the proteasome function. Neurotox Res 2006; 9: 29-37.
[25] Pencheva N, Tran H, Buss C, Huh D, Drobnjak M, Busam K and Tavazoie SF. Convergent multi-miRNA targeting of ApoE drives LRP1/LRP8-dependent melanoma metastasis and angiogenesis. Cell 2012; 151: 1068-1082.
[26] Pennarun G, Chapelin C, Escudier E, Bridoux AM, Dastot F, Cacheux V, Goossens M, Amselem S and Duriez B. The human dynein intermediate chain 2 gene (DNAI2): cloning, mapping, expression pattern, and evaluation as a candidate for primary ciliary dyskinesia. Hum Genet 2000; 107: 642-649.
[27] Diggle CP, Moore DJ, Mali G, zur Lage P, Ait-Lounis A, Schmidts M, Shoemark A, Garcia Munoz A, Halachev MR, Gautier P, Yeyati PL, Bonthron DT, Carr IM, Hayward B, Markham AF, Hope JE, von Kriegsheim A, Mitchison HM, Jackson IJ, Durand B, Reith W, Sheridan E, Jarman AP and Mill P. HEATR2 plays a conserved role in assembly of the ciliary motile apparatus. PLoS Genet 2014; 10: e1004577.
[28] Armstrong DA, Phelps LN and Vincenti MP. CCAAT enhancer binding protein-beta regulates matrix metalloproteinase-1 expression in interleukin-1beta-stimulated A549 lung carcinoma cells. Mol Cancer Res 2009; 7: 1517-1524.
[29] Conca W and Willmroth F. Human T lymphocytes express a member of the matrix metalloproteinase gene family. Arthritis Rheum 1994; 37: 951-956.
[30] McCawley LJ, Crawford HC, King LE Jr, Mudgett J and Matrisian LM. A protective role for matrix metalloproteinase-3 in squamous cell carcinoma. Cancer Res 2004; 64: 6965-6972.
[31] Trump BF and Berezesky IK. Calcium-mediated cell injury and cell death. Faseb J 1995; 9: 219-228.
[32] Toyota M, Ho C, Ohe-Toyota M, Baylin SB and Issa JP. Inactivation of CACNA1G, a T-type calcium channel gene, by aberrant methylation of its 5' CpG island in human tumors. Cancer Res 1999; 59: 4535-4541.
[33] Reis-Filho JS, Steele D, Di Palma S, Jones RL, Savage K, James M, Milanezi F, Schmitt FC and Ashworth A. Distribution and significance of nerve growth factor receptor (NGFR/p75NTR) in normal, benign and malignant breast tissue. Mod Pathol 2006; 19: 307-319.
[34] Hatakeyama S. TRIM proteins and cancer. Nat Rev Cancer 2011; 11: 792-804.
[35] Kung CP, Khaku S, Jennis M, Zhou Y and Murphy ME. Identification of TRIML2, a novel p53 target, that enhances p53 SUMOylation and regulates the transactivation of proapoptotic genes. Mol Cancer Res 2015; 13: 250-262.
[36] Lin ZY, Chuang YH and Chuang WL. Cancer-associated fibroblasts up-regulate CCL2, CCL26, IL6 and LOXL2 genes related to promotion of cancer progression in hepatocellular carcinoma cells. Biomed Pharmacother 2012; 66: 525-529.
[37] Chen G, Rong M and Luo D. TNFRSF6B neutralization antibody inhibits proliferation and induces apoptosis in hepatocellular carcinoma cell. Pathol Res Pract 2010; 206: 631-641.
[38] Zong L, Chen P and Wang DX. Death decoy receptor overexpression and increased malignancy risk in colorectal cancer. World J Gastroenterol 2014; 20: 4440-4445.
[39] Ge Z, Sanders AJ, Ye L, Wang Y and Jiang WG. Expression of death decoy receptor-3 (DcR3) in human breast cancer and its functional effects on breast cancer cells in vitro. J Exp Ther Oncol 2011; 9: 109-118.
[40] Yeo M, Lee SK, Lee B, Ruiz EC, Pfaff SL and Gill GN. Small CTD phosphatases function in silencing neuronal gene expression. Science 2005; 307: 596-600.
[41] Braastad CD, Hovhannisyan H, van Wijnen AJ, Stein JL and Stein GS. Functional characterization of a human histone gene cluster duplication. Gene 2004; 342: 35-40.
[42] Zhang HH, Zhang ZY, Che CL, Mei YF and Shi YZ. Array analysis for potential biomarker of gemcitabine identification in non-small cell lung cancer cell lines. Int J Clin Exp Pathol 2013; 6: 1734-1746.
[43] Barisone GA, Satake N, Lewis C, Duong C, Chen C, Lam KS, Nolta J and Díaz E. Loss of MXD3 induces apoptosis of Reh human precursor B acute lymphoblastic leukemia cells. Blood Cells Mol Dis 2015; 54: 329-335.

[44] Xi Q, Huang M, Wang Y, Zhong J, Liu R, Xu G, Jiang L, Wang J, Fang Z and Yang S. The expression of CDK1 is associated with proliferation and can be a prognostic factor in epithelial ovarian cancer. Tumour Biol 2015; 36: 4939-4948.

[45] Shubbar E, Kovacs A, Hajizadeh S, Parris TZ, Nemes S, Gunnarsdottir K, Einbeigi Z, Karlsson P and Helou K. Elevated cyclin B2 expression in invasive breast carcinoma is associated with unfavorable clinical outcome. BMC Cancer 2013; 13: 1.

[46] Bussey KJ, Bapat A, Linnehan C, Wandoloski M, Dastrup E, Rogers E, Gonzales P and Demeure MJ. Targeting polo-like kinase 1, a regulator of p53, in the treatment of adrenocortical carcinoma. Clin Transl Med 2016; 5: 1.

[47] Vaidyanathan S, Cato K, Tang L, Pavey S, Haass NK, Gabrielli BG and Duijf PH. In vivo overexpression of Emi1 promotes chromosome instability and tumorigenesis. Oncogene 2016; 35: 5446-5455.

[48] Liu X, Wang H, Ma J, Xu J, Sheng C, Yang S, Sun L and Ni Q. The expression and prognosis of Emi1 and Skp2 in breast carcinoma: associated with PI3K/Akt pathway and cell proliferation. Med Oncol 2013; 30: 735.

[49] Sarli V and Giannis A. Targeting the kinesin spindle protein: basic principles and clinical implications. Clin Cancer Res 2008; 14: 7583-7587.

[50] Schaefer-Klein JL, Murphy SJ, Johnson SH, Vasmatzis G and Kovtun IV. Topoisomerase 2 alpha cooperates with androgen receptor to contribute to prostate cancer progression. PLoS One 2015; 10: e0142327.

[51] Votino C, Laudanna C, Parcesepe P, Giordano G, Remo A, Manfrin E and Pancione M. Aberrant BLM cytoplasmic expression associates with DNA damage stress and hypersensitivity to DNA-damaging agents in colorectal cancer. J Gastroenterol 2016; 52: 327-340.

[52] Lin Z, Zhang X, Liu Z, Liu Q, Wang L, Lu Y, Liu Y, Wang M, Yang M, Jin X and Quan C. The distinct expression patterns of claudin-2, -6, and -11 between human gastric neoplasms and adjacent non-neoplastic tissues. Diagnostic Pathology 2013; 8: 133-133.

[53] Arbitrio M, Di Martino MT, Barbieri V, Agapito G, Guzzi PH, Botta C, Iuliano E, Scionti F, Altomare E, Codispoti S, Conforti S, Cannataro M, Tassone P and Tagliaferri P. Identification of polymorphic variants associated with erlotinib-related skin toxicity in advanced non-small cell lung cancer patients by DMET microarray analysis. Cancer Chemother Pharmacol 2016; 77: 205-209.

[54] Rumiato E, Boldrin E, Amadori A and Saggioro D. DMET (Drug-Metabolizing Enzymes and Transporters) microarray analysis of colorectal cancer patients with severe 5-fluorouracil-induced toxicity. Cancer Chemother Pharmacol 2013; 72: 483-488.

[55] Bellezza I, Roberti R, Gatticchi L, Del Sordo R, Rambotti MG, Marchetti MC, Sidoni A and Minelli A. A novel role for Tm7sf2 gene in regulating TNFα expression. PLoS One 2013; 8: e68017.

[56] Bellezza I, Gatticchi L, del Sordo R, Peirce MJ, Sidoni A, Roberti R and Minelli A. The loss of Tm7sf gene accelerates skin papilloma formation in mice. Sci Rep 2015; 5: 9471.

[57] Zhi X, Wang Y, Zhou X, Yu J, Jian R, Tang S, Yin L and Zhou P. RNAi-mediated CD73 suppression induces apoptosis and cell-cycle arrest in human breast cancer cells. Cancer Sci 2010; 101: 2561-2569.

Supplementary Table S1. Selected differentially expressed genes (DEGs) mutually regulated following 10 μM and 15 μM treatment of MS17 in PC-3 cells at 24 hrs

Gene symbol	Genbank accession	Gene description	10 μM	15 μM	*p*-Value	GO term
Up-regulation						
CRYAB+	NM_001885	Crystallin, alpha B	277.6	537.6	5.42E-04	Cytoskeletal organization
HSPA6+	NM_002155	Heat shock 70 kDa protein 6 (HSP70B')	145.2	336.7	1.09E-03	Response to unfolded protein
MAFB	NM_005461	V-maf avian musculoaponeurotic fibrosarcoma oncogene homolog B	49.6	182.9	2.26E-03	Regulation of transcription
RFPL2	NM_006605	Ret finger protein-like 2	49.2	128.8	3.23E-03	Binding activity
NR1H4	NM_005123	Nuclear receptor subfamily 1, group H, member 4	41.6	88.5	5.77E-03	Regulation of transcription
HSPB8+	NM_014365	Heat shock 22 kDa protein 8	41.3	88.4	1.67E-03	Response to unfolded protein
TRIML2+	NM_173553	Tripartite motif family-like 2	30.2	88.1	6.54E-03	Protein ubiquitination
HSPB2	NM_001541	Homo sapiens heat shock 27 kDa protein 2 (HSPB2), mRNA	28.7	77.9	6.17E-03	Response to unfolded protein
KRTAP21-2	NM_181617	Keratin associated protein 21-2	27.9	56.8	1.48E-03	Cytoskeletal organization
INSL4	NM_002195	Insulin-like 4 (placenta)	19.4	54.3	4.87E-03	Cell proliferation
DNAI2+	NM_023036	Dynein, axonemal, intermediate chain 2	24	51.9	7.84E-03	Cytoskeletal organization
CACNA1G+	NM_018896	Calcium channel, voltage-dependent, T type, alpha 1G subunit	17	48.3	2.51E-03	Transporter activity
KRTAP3-2	NM_031959	Keratin associated protein 3-2	18.8	47.9	2.11E-02	Cytoskeletal organization
FABP3	NM_004102	Fatty acid binding protein 3, muscle and heart (mammary-derived growth inhibitor)	19.4	41.2	2.44E-03	Transporter activity
RFPL1	NM_021026	Ret finger protein-like 1	13.3	38.5	4.36E-03	Binding activity
DAZ1	NM_004081	Deleted in azoospermia 1	12.4	37.2	1.38E-02	Reproductive process
MMP3+	NM_002422	Matrix metallopeptidase 3 (stromelysin 1, progelatinase)	15.6	33.9	2.92E-03	Proteolysis
SPANXB2	NM_145664	SPANX family, member B2	20.4	33.6	1.37E-03	Reproductive process
IL10RA	NM_001558	Interleukin 10 receptor, alpha	13.7	32.1	8.38E-03	Immune response
DNAJA4+	NM_018602	DnaJ (Hsp40) homolog, subfamily A, member 4	16.3	31.7	1.55E-03	Protein folding
BATF	NM_006399	Basic leucine zipper transcription factor, ATF-like	12.2	30.3	9.65E-03	Regulation of transcription
GADD45G	NM_006705	Growth arrest and DNA-damage-inducible, gamma	9.9	27	3.07E-03	Apoptosis
SPANXA1	NM_013453	Sperm protein associated with the nucleus, X-linked, family member A1	19.2	27	1.23E-03	Reproductive process
TRIM54	NM_032546	Tripartite motif containing 54	14.9	24.4	1.23E-03	Cytoskeletal organization
HTR3C	NM_130770	5-hydroxytryptamine (serotonin) receptor 3C, ionotropic	10	24.3	4.56E-03	Transporter activity
NGFR+	NM_002507	Nerve growth factor receptor	14.2	23.8	6.34E-03	Apoptosis
CCL26+	NM_006072	Chemokine (C-C motif) ligand 26	13	23.1	1.51E-03	Immune response
DNAJB4	NM_007034	DnaJ (Hsp40) homolog, subfamily B, member 4	10.4	22.2	1.67E-03	Protein folding
RRAD	NM_004165	Ras-related associated with diabetes	8.8	21.4	3.42E-03	Signal transduction
MMP10+	NM_002425	Matrix metallopeptidase 10 (stromelysin 2)	9.2	20.9	6.03E-03	Proteolysis
ABL2	NM_007314	C-abl oncogene 2, non-receptor tyrosine kinase	9.1	18.7	1.24E-03	Cytoskeletal organization
HSPA1L	NM_005527	Heat shock 70 kDa protein 1-like	6.7	18.4	3.21E-03	Response to unfolded protein
LBH	NM_030915	Limb bud and heart development	7.2	18.1	6.54E-03	Regulation of transcription
Down-regulation						
CTDSP1+	NM_021198	CTD (carboxy-terminal domain, RNA polymerase II, polypeptide A) small phosphatase 1	-5.8	-9.3	6.59E-04	Phosphatase activity
MKI67	NM_002417	Marker of proliferation Ki-67	-3.5	-7.6	1.41E-03	Cell proliferation

AURKB	NM_004217	Aurora kinase B	-2.7	-6.6	2.25E-03	Cell cycle
HIST2H3A	NM_001005464	Histone cluster 2, H3a	-4.2	-6.5	9.56E-04	Chromosome organization
NEIL3	NM_018248	Nei endonuclease VIII-like 3 (E. coli)	-2.9	-6.5	2.69E-03	DNA repair
TOP2A	NM_001067	Topoisomerase (DNA) II alpha 170 kDa	-2.5	-6.4	2.95E-03	DNA replication
HLF	NM_002126	Hepatic leukemia factor	-3	-6.4	1.21E-02	Regulation of transcription
CDCA3	NM_031299	Cell division cycle associated 3	-3	-5.8	1.48E-03	Cell cycle
GTSE1	NM_016426	G-2 and S-phase expressed 1	-2.7	-5.8	1.63E-03	Cell cycle
HIST1H1D	NM_005320	Histone cluster 1, H1d	-3.2	-5.7	1.29E-03	Chromosome organization
*HIST1H2AI**	NM_003509	Histone cluster 1, H2ai	-3.7	-5.7	1.66E-03	Chromosome organization
PANX1	NM_015368	Pannexin 1	-3.5	-5.6	2.76E-03	Transporter activity
KIF2C	NM_006845	Kinesin family member 2C	-2.5	-5.3	2.51E-03	Cytoskeletal organization
KIF11	NM_004523	Kinesin family member 11	-3	-5.2	1.63E-03	Cytoskeletal organization
E2F8	NM_024680	E2F transcription factor 8	-2.5	-5.1	4.62E-03	Regulation of transcription
KIF20A	NM_005733	Kinesin family member 20A	-2.5	-5	2.06E-03	Cytoskeletal organization
CDK1	NM_001786	Cyclin-dependent kinase 1	-2.6	-4.9	2.34E-03	Cell cycle
DLGAP5	NM_014750	Discs, large (Drosophila) homolog-associated protein 5	-2.5	-4.9	2.91E-03	Cell proliferation
HIST1H3B	NM_003537	Histone cluster 1, H3b	-3.3	-4.9	1.74E-03	Chromosome organization
ASPM	NM_018136	Asp (abnormal spindle) homolog, microcephaly associated (Drosophila)	-2.6	-4.7	1.41E-03	Cell cycle
FBXO5	NM_001142522	F-box protein 5	-2.8	-4.7	1.88E-03	Cell cycle
HMMR	NM_012484	Hyaluronan-mediated motility receptor	-2.7	-4.6	2.63E-03	Binding activity
CLDN11	NM_005602	Claudin 11	-3	-4.6	1.65E-03	Cell adhesion
*HIST1H2BF**	NM_003522	Histone cluster 1, H2bf	-3.5	-4.6	1.88E-03	Chromosome organization
KIF15	NM_020242	Kinesin family member 15	-2.7	-4.6	1.58E-03	Cytoskeletal organization
TROAP	NM_005480	Trophinin associated protein	-2.3	-4.4	1.41E-03	Cell adhesion
SPC24	NM_182513	SPC24, NDC80 kinetochore complex component	-2.7	-4.4	1.01E-03	Cell cycle
BLM	NM_000057	Bloom syndrome, RecQ helicase-like	-2.4	-4.4	1.53E-03	DNA replication
DEPDC1	NM_017779	DEP domain containing 1	-2.3	-4.4	4.54E-03	Signal transduction
SLFN13	NM_144682	Schlafen family member 13	-3.6	-4.3	3.96E-03	Binding activity
PLK1	NM_005030	Polo-like kinase 1	-2.3	-4.3	6.34E-03	Cell cycle
KIFC1	NM_002263	Kinesin family member C1	-2.2	-4.3	4.47E-03	Cytoskeletal organization
CCNB2	NM_004701	Cyclin B2	-2.4	-4.2	1.86E-03	Cell cycle
HAPLN1	NM_001884	Hyaluronan and proteoglycan link protein 1	-3.2	-4.1	3.19E-02	Cell adhesion
NCAPG	NM_022346	Non-SMC condensin I complex, subunit G	-2.6	-4.1	8.53E-03	Chromosome organization
SLC14A1	NM_001146037	Solute carrier family 14 (urea transporter), member 1 (Kidd blood group)	-2.7	-4.1	1.76E-03	Regulation of transcription
*TNFRSF6B**	NM_003823	Tumor necrosis factor receptor superfamily, member 6b, decoy	-3.4	-4	2.10E-02	Apoptosis
TNS4	NM_032865	Tensin 4	-2.3	-4	2.62E-02	Apoptosis
PRR11	NM_018304	Proline rich 11	-2.5	-4	3.17E-03	Cell cycle
DNAH5	NM_001369	Dynein, axonemal, heavy chain 5	-2.6	-4	1.48E-03	Cytoskeletal organization
NDC80	NM_006101	NDC80 kinetochore complex component	-2.7	-4	1.81E-03	Cytoskeletal organization
E2F2	NM_004091	E2F transcription factor 2	-2	-4	2.23E-03	Regulation of transcription
CENPA	NM_001809	Centromere protein A	-2.3	-3.9	2.63E-03	Cell cycle

MND1	NM_032117	Meiotic nuclear divisions 1 homolog (S. cerevisiae)	-2.4	-3.9	3.16E-03	Cell cycle
ASF1B	NM_018154	Anti-silencing function 1B histone chaperone	-2.3	-3.9	2.06E-03	Chromosome organization
HIST2H2AC	NM_003517	Histone cluster 2, H2ac	-2.9	-3.9	1.63E-03	Chromosome organization
CKAP2L	NM_152515	Cytoskeleton associated protein 2-like	-2.2	-3.9	7.08E-03	Cytoskeletal organization
MMS22L	NM_198468	MMS22-like, DNA repair protein	-2.2	-3.9	2.91E-03	DNA replication
BUB1B	NM_001211	BUB1 mitotic checkpoint serine/threonine kinase B	-2.3	-3.8	1.23E-03	Cell cycle
CASC5	NM_170589	Cancer susceptibility candidate 5	-2.5	-3.8	2.08E-03	Chromosome organization
POC1A	NM_015426	POC1 centriolar protein A	-2.3	-3.8	1.58E-03	Chromosome organization
FANCA	NM_000135	Fanconi anemia, complementation group A	-2.4	-3.8	2.16E-03	DNA repair
NMU	NM_006681	Neuromedin U	-2.5	-3.8	3.05E-03	Signal transduction
RIBC2	NM_015653	RIB43A domain with coiled-coils 2	-2.1	-3.7	2.43E-03	Binding activity
NUF2	NM_145697	NUF2, NDC80 kinetochore complex component	-2.5	-3.7	3.03E-03	Chromosome organization
MXD3[*]	NM_031300	MAX dimerization protein 3	-2.6	-3.7	4.18E-03	Regulation of transcription

[*]Green represents mutually up-regulated genes while red indicates mutually down-regulated genes in DU145 cells.

Supplementary Table S2. Selected differentially expressed genes (DEGs) mutually regulated following 10 μM and 15 μM treatment of MS17 in DU145 cells at 24 hrs

Gene symbol	Genbank accession	Gene description	10 μM	15 μM	*p*-Value	GO term
Up-regulation						
HSPA6[*]	NM_002155	Heat shock 70 kDa protein 6 (HSP70B')	373.4	814.4	4.96E-04	Response to unfolded protein
CRYAB[*]	NM_001885	Crystallin, alpha B	334.9	493.9	5.46E-04	Cytoskeletal organization
MMP10[*]	NM_002425	Matrix metallopeptidase 10 (stromelysin 2)	96.7	165.2	5.11E-03	Proteolysis
MMP3[*]	NM_002422	Matrix metallopeptidase 3 (stromelysin 1, progelatinase)	71.6	122.8	5.83E-03	Proteolysis
CCL26[*]	NM_006072	Chemokine (C-C motif) ligand 26	56	81.4	1.70E-03	Immune response
CACNA1G[*]	NM_018896	Calcium channel, voltage-dependent, T type, alpha 1G subunit	23	60.2	3.60E-02	Transporter activity
NGFR[*]	NM_002507	Nerve growth factor receptor	31.5	53.6	1.15E-02	Apoptosis
DEFB103B	NM_018661	Defensin, beta 103B	54.7	50.9	5.57E-04	Immune response
ATF3	NM_001040619	Activating transcription factor 3	28.7	45.7	1.48E-03	Regulation of transcription
MMP1	NM_002421	Matrix metallopeptidase 1 (interstitial collagenase)	37.3	43.1	1.32E-03	Proteolysis
ZNF556	NM_024967	Zinc finger protein 556	22	41.3	1.46E-02	Regulation of transcription
KRT14	NM_000526	Keratin 14	17.7	36.1	2.51E-03	Structural molecule activity
DNAI2[*]	NM_023036	Dynein, axonemal, intermediate chain 2	17.6	32.1	3.77E-02	Cytoskeletal organization
NRAP	NM_198060	Nebulin-related anchoring protein	15.2	29.5	3.60E-02	Binding activity
KRT34	NM_021013	Keratin 34	17.8	25.4	5.36E-03	Structural molecule activity
TRIML2[*]	NM_173553	Tripartite motif family-like 2	11.6	24.7	3.61E-02	Protein ubiquitination
PGF	NM_002632	Placental growth factor	13.1	24	1.54E-02	Angiogenesis
SDCBP2	NM_080489	Syndecan binding protein (syntenin) 2	14.3	21.6	4.40E-04	Binding activity
RFPL4AL1	NM_001277397	Ret finger protein-like 4A-like 1	11	19.8	2.58E-02	Binding activity
HEY1	NM_001040708	Hes-related family bHLH transcription factor with YRPW motif 1	9.3	19.8	4.48E-02	Regulation of transcription

*DNAJA4**	NM_018602	DnaJ (Hsp40) homolog, subfamily A, member 4	11.5	19.1	3.87E-03	Protein folding
CHST1	NM_003654	Carbohydrate (keratan sulfate Gal-6) sulfotransferase 1	11.4	18.8	2.23E-03	Metabolic process
ZNF844	NM_001136501	Zinc finger protein 844	11.6	18	1.37E-02	Regulation of transcription
*HSPB8**	NM_014365	Heat shock 22 kDa protein 8	12	18	2.89E-02	Response to unfolded protein
SCN3B	NM_018400	Sodium channel, voltage-gated, type III, beta subunit	9	17.6	3.74E-02	Transporter activity
DHRS2	NM_182908	Dehydrogenase/reductase (SDR family) member 2	11.5	16.7	6.31E-03	Oxidoreductase activity
ARHGEF7	NM_145735	Rho guanine nucleotide exchange factor (GEF) 7	10.4	16.7	1.44E-02	Signal transduction activity
SERPIND1	NM_000185	Serpin peptidase inhibitor, clade D (heparin cofactor), member 1	11.6	16.5	2.10E-02	Endopeptidase activity
AQP1	NM_198098	Aquaporin 1 (Colton blood group)	10.6	16.5	9.07E-03	Transporter activity
SYNPO2L	NM_024875	Synaptopodin 2-like	9	16.1	2.58E-02	Cytoskeletal organization
GCGR	NM_000160	Glucagon receptor	10.5	15.9	3.01E-02	Signal transduction activity
MAL	NM_002371	Mal, T-cell differentiation protein	7.5	15.8	3.18E-02	Apoptosis
Down-regulation						
*TNFRSF6B**	NM_003823	Tumor necrosis factor receptor superfamily, member 6b, decoy	-4.5	-6.5	3.66E-03	Apoptosis
*CTDSP1**	NM_021198	CTD (carboxy-terminal domain, RNA polymerase II, polypeptide A) small phosphatase 1	-4.7	-5.8	6.10E-03	Phosphatase activity
DGAT2	NM_032564	Diacylglycerol O-acyltransferase 2	-3.6	-4.6	1.16E-02	Metabolic process
LHX3	NM_014564	LIM homeobox 3	-2.5	-4.5	6.56E-03	Regulation of transcription
DTX4	NM_015177	Deltex homolog 4 (Drosophila)	-4.1	-4.2	1.39E-03	Cell cycle
B9D1	NM_015681	B9 protein domain 1	-2.9	-3.7	1.32E-03	Receptor activity
*HIST1H2BF**	NM_003522	Histone cluster 1, H2bf	-2.7	-3.3	2.38E-02	Chromosome organization
CYP24A1	NM_000782	Cytochrome P450, family 24, subfamily A, polypeptide 1	-2.9	-3.3	2.07E-02	Oxidoreductase activity
LOXL2	NM_002318	Lysyl oxidase-like 2	-2.7	-3.2	2.88E-02	Oxidoreductase activity
PRKAG1	NM_001206710	Protein kinase, AMP-activated, gamma 1 non-catalytic subunit	-2.4	-3.2	1.59E-02	Protein kinase activity
RAB26	NM_014353	RAB26, member RAS oncogene family	-2.4	-3.1	1.53E-02	Signal transduction activity
MPZL2	NM_144765	Myelin protein zero-like 2	-2.3	-3	1.59E-02	Cell adhesion
PARD6A	NM_016948	Par-6 family cell polarity regulator alpha	-2.5	-3	4.28E-02	Cell cycle
PHYHD1	NM_174933	Phytanoyl-CoA dioxygenase domain containing 1	-2.3	-3	1.97E-02	Oxidoreductase activity
MAP2K6	NM_002758	Mitogen-activated protein kinase kinase 6	-2.4	-3	7.31E-03	Protein kinase activity
ARHGEF9	NM_015185	Cdc42 guanine nucleotide exchange factor (GEF) 9	-2.4	-3	6.02E-03	Signal transduction activity
HOXC4	NM_014620	Homeobox protein Hox-C4	-2.7	-2.9	8.29E-03	Regulation of transcription
STMN3	NM_015894	Stathmin-like 3	-2.5	-2.8	2.91E-02	Binding activity
*HIST1H2AI**	NM_003509	Histone cluster 1, H2ai	-2.6	-2.8	3.15E-03	Chromosome organization
B3GNT4	NM_030765	UDP-GlcNAc:betaGal beta-1,3-N-acetylglucosaminyltransferase 4	-2.1	-2.8	3.52E-02	Metabolic process
GABRD	NM_000815	Gamma-aminobutyric acid (GABA) A receptor, delta	-2.3	-2.8	3.86E-03	Signal transduction activity
TBCD	NM_005993	Tubulin folding cofactor D	-2.3	-2.7	2.95E-02	Binding activity
CLEC11A	NM_002975	C-type lectin domain family 11, member A	-2.2	-2.7	2.45E-02	Cell proliferation
PADI2	NM_007365	Peptidyl arginine deiminase, type II	-2.6	-2.7	1.44E-02	Chromosome organization
PTGDS	NM_000954	Prostaglandin D2 synthase 21 kDa (brain)	-2.3	-2.7	1.10E-02	Metabolic process
NT5E	NM_002526	5'-nucleotidase, ecto (CD73)	-2	-2.7	3.94E-04	Metabolic process
ALDH3A1	NM_001135168	Aldehyde dehydrogenase 3 family, member A1	-2	-2.7	3.23E-02	Oxidoreductase activity
PAQR4	NM_152341	Progestin and adipoQ receptor family member IV	-2.4	-2.7	2.84E-03	Receptor activity

*MXD3**	NM_031300	MAX dimerization protein 3	-2	-2.7	1.02E-02	Regulation of transcription
WWC3	NM_015691	WWC family member 3	-2.1	-2.7	5.95E-03	Regulation of transcription
NAT14	NM_020378	N-acetyltransferase 14 (GCN5-related, putative)	-2.3	-2.7	1.10E-02	Transferase activity
MTFP1	NM_016498	Mitochondrial fission process 1	-2.7	-2.6	2.58E-02	Apoptosis
EGFL7	NM_201446	EGF like Domain Multiple 7	-2.4	-2.6	3.86E-04	Binding activity
CCDC80	NM_199511	Coiled-coil domain containing 80	-2	-2.6	5.32E-03	Binding activity
LTBP2	NM_000428	Latent transforming growth factor beta binding protein 2	-2.1	-2.6	2.47E-02	Cell adhesion
TM7SF2	NM_003273	Transmembrane 7 superfamily member 2	-2.2	-2.6	1.42E-03	Metabolic process
GRHPR	NM_012203	Glyoxylate reductase/hydroxypyruvate reductase	-2.3	-2.6	2.28E-03	Oxidoreductase activity
DHRS4	NM_001282989	Dehydrogenase/reductase (SDR family) member 4	-2.2	-2.6	2.97E-02	Oxidoreductase activity
MAMDC4	NM_206920	MAM domain containing 4	-2.3	-2.6	4.69E-03	Transporter activity
SYTL2	NM_206927	Synaptotagmin-like 2	-2.2	-2.6	3.51E-02	Transporter activity
KCNMA1	NM_002247	Potassium large conductance calcium-activated channel, subfamily M, alpha member 1	-2.1	-2.6	1.19E-02	Transporter activity
NCKIPSD	NM_016453	NCK interacting protein with SH3 domain	-2.1	-2.5	1.52E-02	Binding activity
NUDT8	NM_001243750	Nudix (nucleoside diphosphate linked moiety X)-type motif 8	-2.2	-2.5	8.33E-03	Metabolic process
LOXL1	NM_005576	Lysyl oxidase-like 1	-2.3	-2.5	1.16E-03	Oxidoreductase activity
LY9	NM_001033667	Lymphocyte antigen 9	-2	-2.5	3.55E-03	Protein kinase activity
SFRP1	NM_003012	Secreted frizzled-related protein 1	-2.1	-2.5	6.84E-03	Receptor activity
SPDEF	NM_012391	SAM pointed domain containing ETS transcription factor	-2.2	-2.5	1.14E-02	Regulation of transcription
ARHGDIB	NM_001175	Rho GDP dissociation inhibitor (GDI) beta	-2.2	-2.5	2.61E-03	Signal transduction activity
SLC27A5	NM_012254	Solute carrier family 27 (fatty acid transporter), member 5	-2.2	-2.5	6.01E-04	Transporter activity

*Green represents mutually up-regulated genes while red indicates mutually down-regulated genes in PC-3 cells.